Supporting Information for

Interlayer Polarization Induced by Ag-N_2 Motifs in Spherical Covalent Organic Framework Driving Efficient CO_2 Photoreduction

Yueling Chen[a,b], Shibin Zheng[b], Xingci Huang[b], Zhangtong Zhang[b], Guocheng Huang[b], Qiaoshan Chen[b], Ling Wu[a], and Jinhong Bi[a,b]*

[a] *State Key Laboratory of Photocatalysis on Energy and Environment, College of Chemistry, Fuzhou University, Minhou, Fujian 350108, China*

[b] *Department of Environmental Science and Engineering, Fuzhou University, Minhou, Fujian 350108, China*

*Corresponding author:

E-mail address: bijinhong@fzu.edu.cn

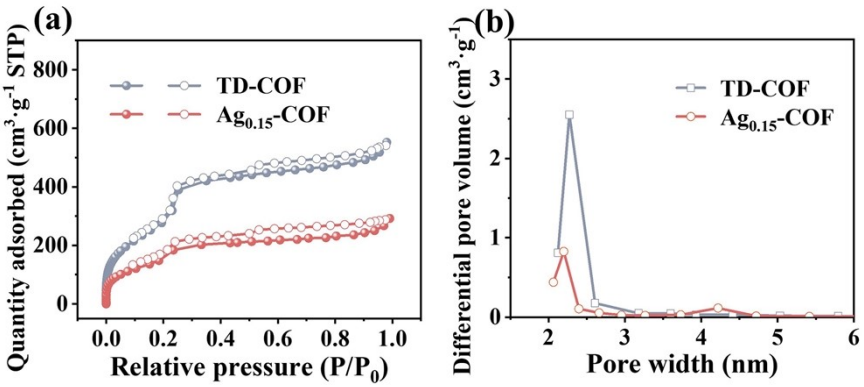

Fig. S1. Nitrogen adsorption and desorption curves of TD-COF and $Ag_{0.15}$-COF at low temperatures.

Table S1. Pore volume, average pore size, BET surface area of prepared catalysts.

Sample	Pore volume ($cm^3 \cdot g^{-1}$)	Average pore size (nm)	BET surface area ($m^2 \cdot g^{-1}$)
TD-COF	0.90	2.27	1159.84
$Ag_{0.15}$-COF	0.38	2.06	651.17

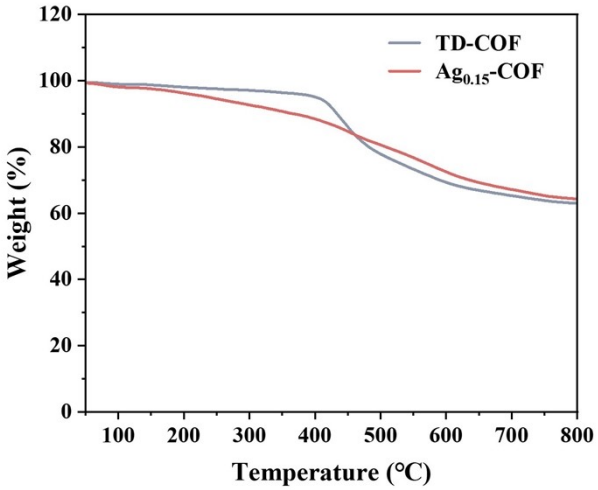

Fig. S2. The TGA curves of TD-COF and $Ag_{0.15}$-COF.

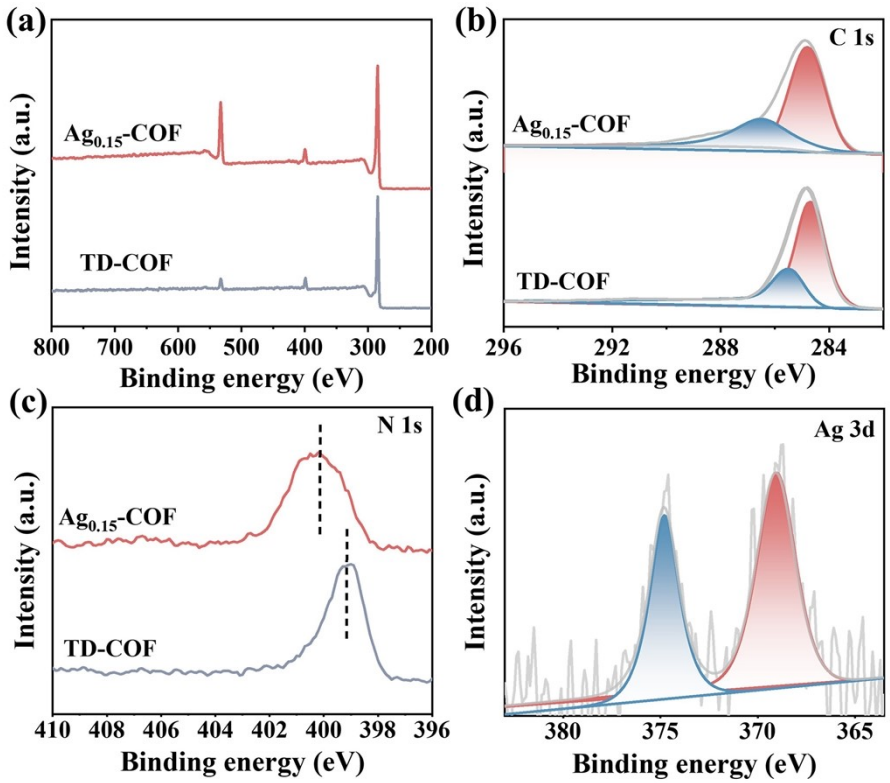

Fig. S3. (a) XPS survey spectra for samples spectrum. XPS spectra of (b) C 1s, and (c) N 1s in TD-COF and $Ag_{0.15}$-COF. (d) XPS spectra of Ag 3d in $Ag_{0.15}$-COF.

Table S2. EXAFS fitting parameters at the Ag K-edge ($S_0^2 = 0.823$).

Sample	Shell	CN[a]	*R* (Å)[b]	σ^2 (Å^2)[c]	ΔE_0 (eV)[d]	*R* factor
Ag-foil	Ag-Ag	12	2.861 ± 0.002	0.0093 ± 0.0002	2.4 ± 0.2	0.0023
Ag_2O	Ag-O	1.2 ± 0.1	2.049 ± 0.001	0.0049 ± 0.0008	0.6 ± 0.4	0.0028
	Ag-O	0.5 ± 0.1	2.444 ± 0.001			
	Ag-Ag	2.7 ± 0.5	3.324 ± 0.001	0.0237 ± 0.0033	2.2 ± 0.4	
Ag-COF	Ag-N	1.7 ± 0.1	2.108 ± 0.001	0.0015 ± 0.0011	4.2 ± 0.1	0.0085
	Ag-C	0.4 ± 0.1	2.284 ± 0.001			

a: coordination number; *b*: the distance to the neighboring atom; *c*: the mean square relative displacement; *d*: inner potential correction.

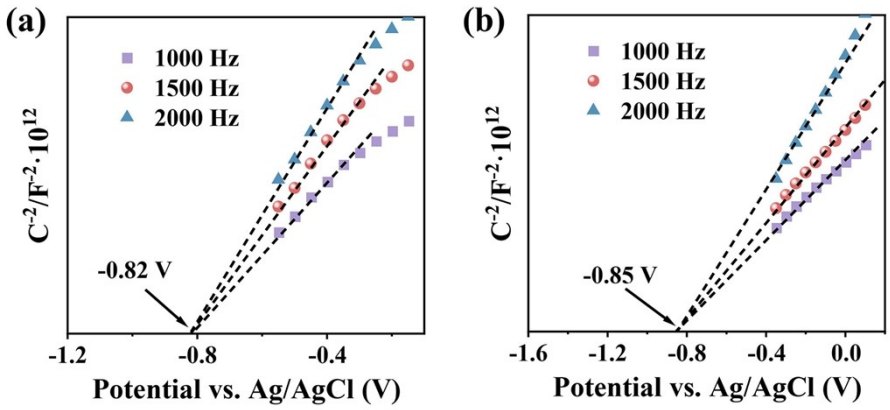

Fig. S4. Mott-Schottky plots of (a) TD-COF and (b) $Ag_{0.15}$-COF.

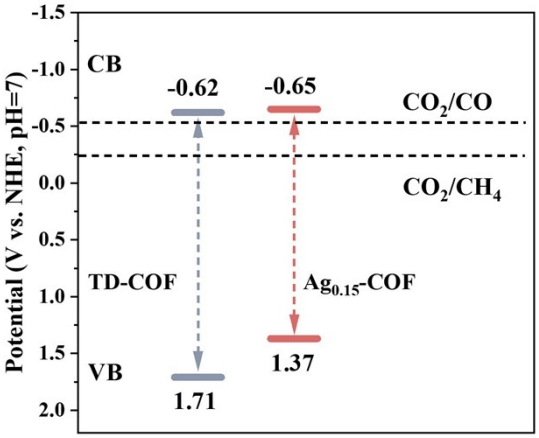

Fig. S5. The band structure of TD-COF and $Ag_{0.15}$-COF.

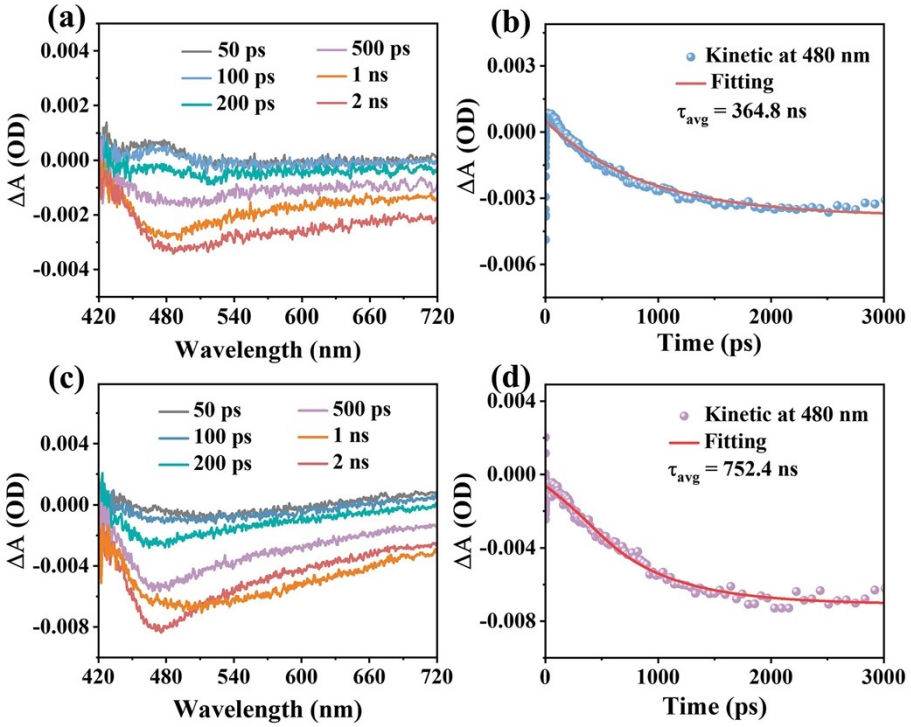

Fig. S6. Fs-TAs of (a) TD-COF and (c) $Ag_{0.15}$-COF. Normalized fs-TAs kinetics at 480 nm for (b) TD-COF and (d) $Ag_{0.15}$-COF.

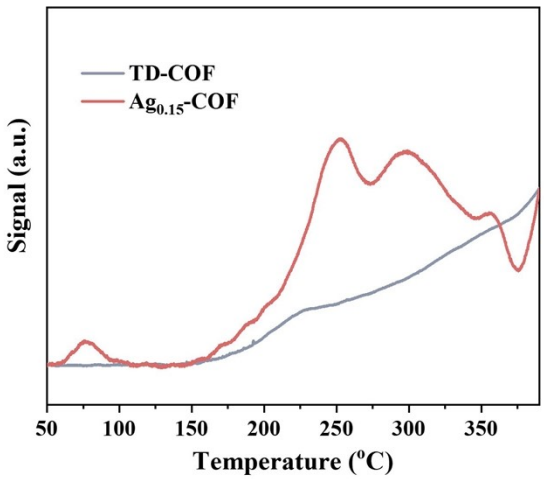

Fig. S7. CO_2-TPD spectra of TD-COF and $Ag_{0.15}$-COF.

Table S3. The photocatalytic CO_2 reduction performance of TD-COF and Ag_x-COF samples.

Catalyst	CO (μmol·L^{-1})	CH_4 (μmol·L^{-1})	CO (μmol·g^{-1}·h^{-1})	CH_4 (μmol·g^{-1}·h^{-1})	CO selectivity (%)
TD-COF	19.22	0.40	2.10	0.10	95.45
$Ag_{0.05}$-COF	68.27	0.84	7.46	0.21	97.26
$Ag_{0.10}$-COF	142.50	0.88	15.57	0.22	98.61
$Ag_{0.15}$-COF	184.05	0.96	20.11	0.24	98.82
$Ag_{0.20}$-COF	105.80	0.64	11.56	0.16	98.63
$Ag_{0.30}$-COF	53.72	0.52	5.87	0.13	97.83

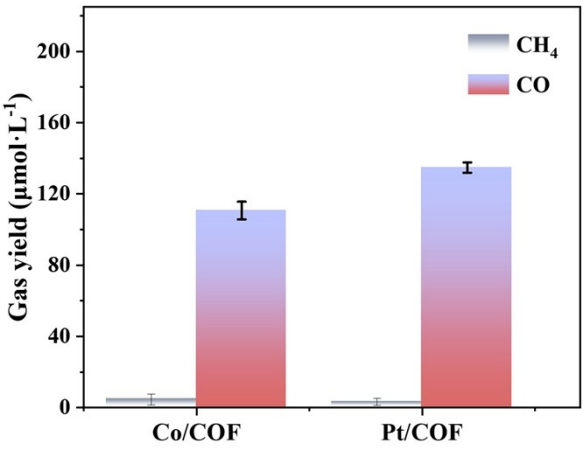

Fig. S8. The photocatalytic CO_2 performance of Co/COF and Pt/COF.

Table S4. Comparison with the photocatalytic activity of materials in recent years.

Catalysts	Reaction condition	Light source	Yield of CO (μmol·L^{-1})	Ref.
$Ag_{0.15}$/COF	Water	300 W Xe lamp (420-800 nm)	184.05	This work
Pd_3/Py-bTDC	Water	300 W Xe lamp (420-800 nm)	40.61	1
TTCOF-Zn	Water	300 W Xe lamp (420-800 nm)	4.81	2
$CuWO_4$/TTCOF	Water	300 W Xe lamp (420-800 nm)	16.40	3
ZnInS/CuS	Water	300 W Xe lamp	30.54	4
HUS-7	TEOA and water	UVC 254 nm	32.03	5
$In_4SnS_8/Cs_3Bi_2Br_9$	Water	300 W Xe lamp	21.85	6
CO_2-Zr_{12}-DEPB	Acetonitrile and 0.1 mL water	300 W Xe lamp	38.26	7
$TiO_2/BiVO_4$-4	Water	Xe lamp	39.65	8
B_4C	Water	300 W Xe lamp	3.91	9
BiOBr/TCN	Water	300 W Xe lamp	24.92	10

Table S5. Rate of CO evolution and apparent quantum efficiency of $Ag_{0.15}$/COF at 450 nm.

Wavelength (nm)	Light intensity ($mW \cdot cm^2$)	Yield of CO ($\mu mol \cdot h^{-1}$)	AQE (%)
450	9.6	11.46	0.058

$$AQY\ (\%) = \frac{\text{the number of evolved CO molecules} \times 2}{\text{the number of incident photons}} \times 100\%$$

$$= \frac{2 \times N_A \times M_{CO}}{\frac{E\lambda}{hc}} \times 100\% = \frac{2 \times N_A \times M_{CO}}{\frac{P \times a \times T \times \lambda}{hc}} \times 100\%$$

$$= \frac{2 \times 6.022 \times 10^{23} \times 11.46 \times 10^{-7} \times 6.63 \times 10^{-34} \times 3 \times 10^{8}}{9.60 \times 3 \times 10^{-4} \times 60 \times 60 \times 450 \times 10^{-9}} \times 100\%$$

$$= 0.058\%$$

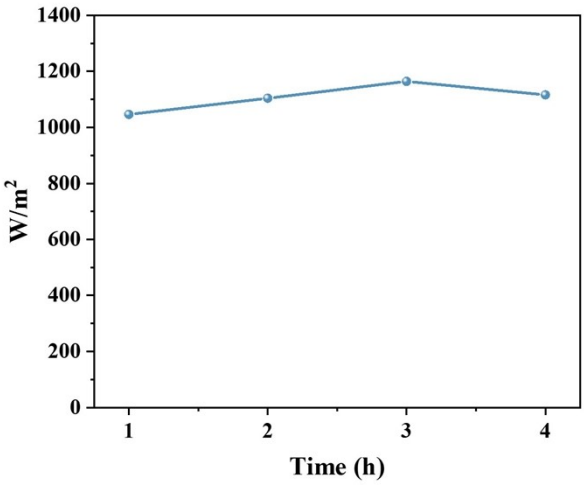

Fig. S9. The actual light intensity of sunlight in photocatalytic CO_2 reduction experiments.

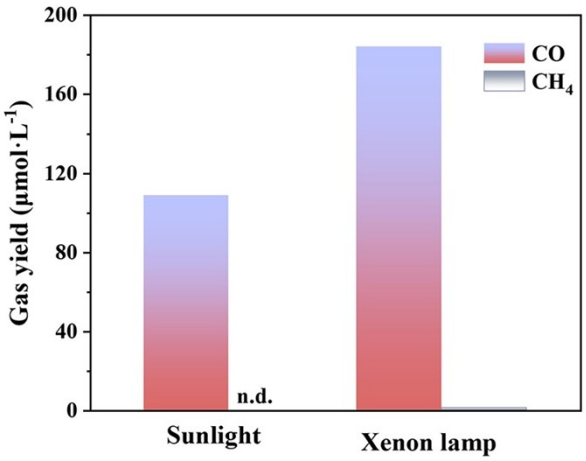

Fig. S10. Photocatalytic CO_2 reduction activities of $Ag_{0.15}$-COF under sunlight and xenon lamp, respectively.

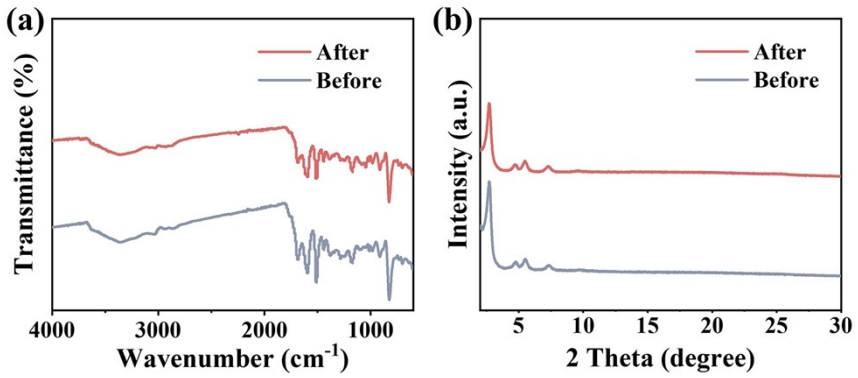

Fig. S11. (a) XRD and (b) FT-IR spectra of $Ag_{0.15}$-COF before and after cyclic reaction.

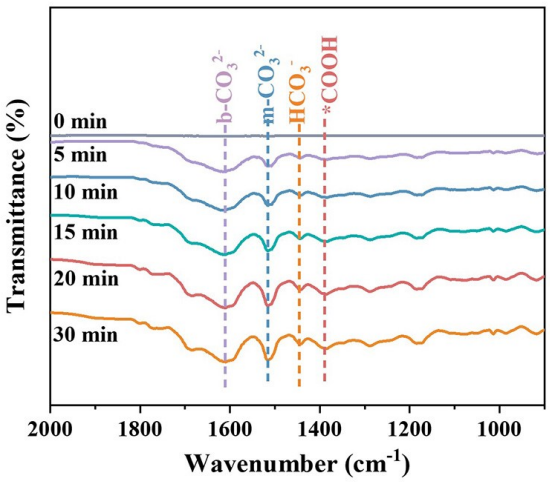

Fig. S12. *In-situ* FTIR of $Ag_{0.15}$-COF.

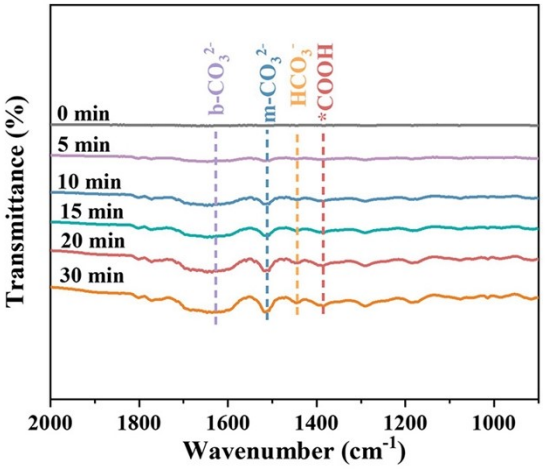

Fig. S13. *In-situ* FTIR of TD-COF.

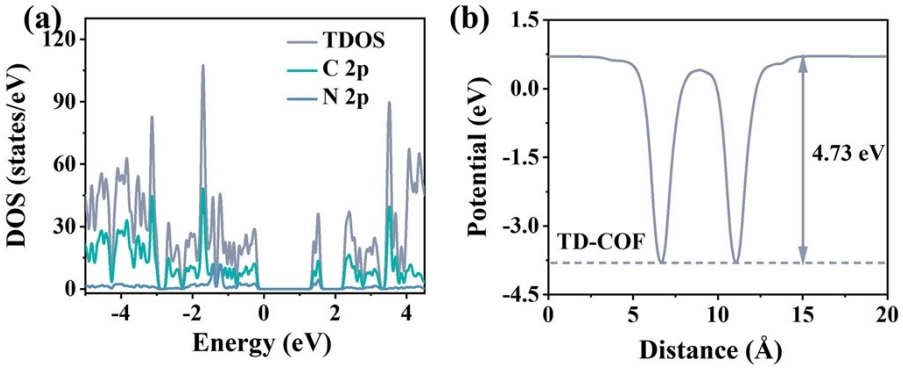

Fig. S14. Calculated (a) projected density of states and (b) electrostatic potential along the interlayer direction of $Ag_{0.15}$-COF.

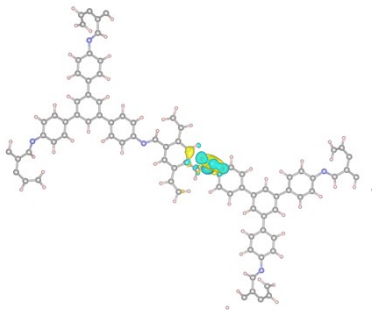

Fig. S15. Charge density difference for CO_2 adsorption on TD-COF. Yellow and blue denote electron accumulation and depletion, respectively.

References

1 Y. Lin, X. Lai, G. Huang, J. Luo, Q. Chen, G. Huang, J. Bi, *Chem. Eur. J.*, 2025, **31**, e202500766.

2 M. Lu, J. Liu, Q. Li, M. Zhang, M. Liu, J.L. Wang, D.Q. Yuan, Y.Q. Lan, *Angew. Chem. Int. Ed.*, 2019, **58**, 12392-12397.

3 Q. Niu, S. Dong, J. Tian, G. Huang, J. Bi, L. Wu, *ACS Appl. Mater. Interfaces*, 2022, **14**, 24299-24308.

4 C. Yan, M. Xu, J. Li, H. Wang, P. Huo, *Fuel*, 2024, **378**, 132921.

5 R. Ricka, T. W. M. Amen, N. Tsunoji, M. Reli, M. Filip Edelmannová, M. Kormunda, M. Ritz, K. Kočí, *ChemSusChem*, 2024, **17**, e202400434.

6 Z. Zhang, M. Wang, Z. Chi, W. Li, H. Yu, N. Yang, H. Yu, *Appl. Catal. B Environ. Energy*, 2022, *313*, 121426.

7 B. Song, W. Song, Y. Liang, Y. Liu, B. Li, H. Li, L. Zhang, Y. Ma, R. Ye, B.Z. Tang, D. Zhao, Y. Zhou, B. Liu, *Angew. Chem. Int. Ed.*, 2025, **64**, e202421248.

8 C. Chen, M. Wu, Y. Xu, C. Ma, M. Song, G. Jiang, *J. Am. Chem. Soc.*, 2024, **146**, 9163-9171.

9 D. Yan, J. Liu, X. Fu, P. Liu, H. Luo, *J. Mater. Sci.*, 2019, **54**, 6151-6163.

10 W. Tao, Q. Tang, J. Hu, Z. Wang, B. Jiang, Y. Xiao, R. Song, S. Guo, *J. Mater. Chem. A*, 2023, **11**, 24999-25007.